

# Influence of polyethylene glycol coating on biodistribution and toxicity of nanoscale graphene oxide in mice after intravenous injection

Bo Li<sup>1,2</sup>

Xiao-Yong Zhang<sup>1</sup>

Jian-Zhong Yang<sup>1</sup>

Yu-Jie Zhang<sup>1</sup>

Wen-Xin Li<sup>1</sup>

Chun-Hai Fan<sup>1</sup>

Qing Huang<sup>1</sup>

<sup>1</sup>Laboratory of Physical Biology, Shanghai Institute of Applied Physics, Chinese Academy of Sciences, Shanghai, <sup>2</sup>Department of Human Anatomy, College of Basic Medical Sciences, Jilin University, Changchun, People's Republic of China

**Abstract:** In this study, we assessed the in vivo behavior and toxicology of nanoscale graphene oxide (NGO) in mice after intravenous injection. The influence of a polyethylene glycol (PEG) coating on the distribution and toxicity of the NGO was also investigated. The results show that NGO is mainly retained in the liver, lung, and spleen. Retention in the lung is partially due to NGO aggregation. The PEG coating reduces the retention of NGO in the liver, lung, and spleen and promotes the clearance of NGO from these organs, but NGO and NGO-PEG are still present after 3 months. The PEG coating effectively reduces the early weight loss caused by NGO and alleviates NGO-induced acute tissue injuries, which can include damage to the liver, lung, and kidney, and chronic hepatic and lung fibrosis.

**Keywords:** graphene oxide, biodistribution, toxicity, polyethylene glycol

## Introduction

Nanoscale graphene oxide (NGO) consists of oxidized graphene sheets with abundant functional groups on their surface that make NGO soluble in water and provide opportunities for chemical modification.<sup>1–5</sup> As a nascent nanomaterial, NGO exhibits unique size, shape, and physicochemical properties that make it a promising biomaterial for biomedical applications.<sup>6–10</sup> Recently, NGO has been demonstrated to be an effective nanocarrier of anticancer drugs.<sup>11–14</sup> However, the in vivo distribution and toxicity of NGO, which would provide important supporting information to help determine its feasibility for potential biomedical applications, have rarely been evaluated.

Polyethylene glycol (PEG) is a commonly used biocompatible polymer that has been used to increase the solubility, reduce the accumulation in the mononuclear phagocyte system (MPS), and prolong the blood half-life of various nanoparticles and nanoparticle complexes.<sup>15–20</sup> PEG is fixed on nanoparticle surfaces by adsorption or covalent binding. When functionalized with PEG, nanoparticles can avoid serum protein binding and achieve enhanced permeability and retention in tumor model systems.<sup>21,22</sup> It has been reported that PEGylated NGO with a size range of 10–50 nm exhibits highly efficient passive tumor targeting with relatively low retention in the MPS and no obvious side effects.<sup>23</sup> However, a comparative study of the distribution and toxicity of NGO with or without PEG coating has not been reported until now, especially for larger-size graphene oxide.

In this study, the in vivo behavior of NGO in mice after intravenous injection was investigated using <sup>125</sup>I radioisotope tracing. In addition, the toxicology of NGO was determined using an evaluation system that includes the assessment of body weight, a blood biochemistry analysis, and a histopathological examination. We particularly

Correspondence: Qing Huang  
Laboratory of Physical Biology,  
Shanghai Institute of Applied Physics,  
Chinese Academy of Sciences,  
PO Box 800-204, Shanghai 201800,  
People's Republic of China  
Tel +86 21 3919 4520  
Fax +86 21 3919 4520  
Email huangqing@sinap.ac.cn

focused on the influence of the PEG coating on the distribution and toxicity of NGO.

## Materials and methods

### Materials

Carrier-free  $\text{Na}^{125}\text{I}$  was purchased from PerkinElmer (Waltham, MA, USA), chloramine-T was sourced from Merck Chemicals Co., Ltd. (Shanghai, People's Republic of China), and the other chemicals were supplied by Sinopharm Chemical Reagent Co., Ltd. (Shanghai, People's Republic of China). The synthesis and characterization of NGO and  $^{125}\text{I}$ -NGO was performed as previously described.<sup>24</sup> NGO was synthesized from natural graphite by oxidation with  $\text{H}_2\text{SO}_4/\text{KMnO}_4$  according to a modified Hummers method. The NGO was characterized by Fourier transform infrared spectroscopy (Avatar 370; Thermo Fisher Scientific Inc., Waltham, MA, USA), Raman spectroscopy (LabRam-1B; JY Co., Ltd., Dilor, France), scanning electron microscopy (1530VP; LEO Corporation, Oberkochen, Germany), transmission electron microscopy (JEOL 2010; JEOL Ltd., Tokyo, Japan), and atomic force microscopy (Nanoscope III; Veeco Metrology Group, Santa Barbara, CA, USA).  $^{125}\text{I}$ -NGO was synthesized according to the chloramine-T (N-chloro-p-toluenesulfonic acid) method. The radiochemical purity and stability of  $^{125}\text{I}$ -NGO was then examined.

### PEG coating

Normal saline (0.9%) was added to the NGO or  $^{125}\text{I}$ -NGO suspension at a 1:1 ratio. The mixture was centrifuged at 14,000 rpm for 5 minutes, decanted, and resuspended in 2 mg/mL PEG6000 (linear, without any functional group at its end) solution. After incubation under ultrasonication for 30 minutes at room temperature, 0.9% normal saline was added again, and the mixture was centrifuged at 14,000 rpm for 5 minutes, decanted, and resuspended in Milli-Q water. After ultrasonication for 30 minutes at room temperature, the same procedure was repeated three times to remove excess PEG reagent. The resultant PEG-modified NGO was designated as NGO-PEG or  $^{125}\text{I}$ -NGO-PEG, respectively. Meanwhile, NGO and  $^{125}\text{I}$ -NGO suspension without PEG coatings were also prepared by the same method, except that Milli-Q water was substituted for PEG6000 solution. Thermal gravimetric analysis of NGO and NGO-PEG was performed to determine the amount of PEG coating layer on the surface of the NGO using a thermal gravimetric analyzer (TG 209 F3 Tarsus; Netzsch, Selb, Germany). The temperature of the sample was gradually increased from 40°C to 700°C at a rate

of 10°C per minute. In addition, the size, polydispersity index, and zeta potential of NGO and NGO-PEG in Milli-Q water were measured by dynamic light scattering with a DelsaNano C particle analyzer (A53878; Beckman Coulter Inc., Indianapolis, IN, USA).

### Animals

All animal experiments were performed in compliance with the national guidelines for the care and use of experimental animals. The protocol was approved by the ethics committee of Shanghai Institute of Applied Physics, Chinese Academy of Sciences (Number 2011-0016). Male Kunming mice (28–32 g) were obtained from the Shanghai Slack Experimental Animal Center. The animal room was maintained at 22°C with a daily light-dark cycle (with light from 6 am to 6 pm). The mice were fed standard mouse chow and provided water ad libitum. All of the procedures using animals were reviewed and approved by the Institutional Animal Care and Use Committee.

### Distribution of $^{125}\text{I}$ -NGO, $^{125}\text{I}$ -NGO-PEG, and $\text{Na}^{125}\text{I}$

Eighty mice were randomly assigned to 16 groups (five mice per group). Each mouse was intravenously injected with 100  $\mu\text{L}$  of  $^{125}\text{I}$ -NGO,  $^{125}\text{I}$ -NGO-PEG, or  $\text{Na}^{125}\text{I}$  through a tail vein. The mice were sacrificed at different time points. The blood was collected and weighed. The tissues, including thyroid gland, heart, lungs, liver, spleen, kidneys, stomach (emptied), small intestine (full), and large intestine (full) were immediately dissected and washed. Each tissue was wrapped in aluminum foil and counted for  $^{125}\text{I}$  radioactivity on the  $\gamma$  detector. Data were corrected for physical decay of radioactivity.

The distribution of the injected sample in the blood and in each organ was represented as the percentage of the injected dose (sample activity/total activity injected). The blood concentrations of NGO and NGO-PEG were represented by the percentage of the injected dose per gram. The blood circulation half-lives of  $^{125}\text{I}$ -NGO and  $^{125}\text{I}$ -NGO-PEG were calculated using 3P97 pharmacokinetic software based on the blood concentrations of  $^{125}\text{I}$ -NGO and  $^{125}\text{I}$ -NGO-PEG at 10 minutes, 30 minutes, one hour, 3 hours, 6 hours, 12 hours, and 24 hours.

### Toxicology evaluation

Sixty mice were randomly assigned to three groups (20 mice per group). Each mouse was intravenously injected with Milli-Q water, 5 mg/kg NGO, or 5 mg/kg NGO-PEG through a tail vein. The mice were sacrificed at 24 hours, one week,

one month, and 3 months (five mice per time point per group). Evaluation included assessment of body weight, a blood biochemical analysis, and a histopathological examination.

## Blood biochemical analysis

The mice were exsanguinated and sacrificed by removal of the eyeballs following anesthesia with an intraperitoneal injection of 0.1 mL of pentobarbital sodium (50 mg/kg). Approximately 0.8 mL of blood from each mouse was collected. The blood samples were centrifuged at 2,000 rpm for 5 minutes, and sera were collected for biochemical analysis. The serum levels of alanine aminotransferase, aspartate aminotransferase, creatinine, alkaline phosphatase, blood urea nitrogen, uric acid, total protein, albumin, and globulin were evaluated using a clinical automatic chemistry analyzer (Type 7170A; Hitachi Ltd., Tokyo, Japan).

## Histopathological examination

After the mice were exsanguinated and sacrificed by removal of the eyeballs, the major organs, including the liver, lung, and spleen, were excised and fixed in 4% paraformaldehyde for at least 7 days before further processing. These organs were then embedded in paraffin, thin-sectioned at 5  $\mu$ m, and mounted on glass microscope slides using standard histopathological techniques. The sections were stained with hematoxylin-eosin or Masson's trichrome and examined by optical microscopy (Axioskop 2 plus; Carl Zeiss, Poughkeepsie, NY, USA).

## Statistical analysis

The statistical analysis was conducted using Statistical Package for the Social Sciences PASW Statistics version 18 software (SPSS Inc., Chicago, IL, USA), and all of the data are expressed as the mean  $\pm$  standard error of the mean. A one-way analysis of variance followed by Dunnett's post test was performed to determine the statistical significance ( $P < 0.05$ ) between the indicated groups.

## Results

### Materials

The Fourier transform infrared spectrum of NGO showed the most characteristic features of graphene oxide: O-H stretching vibrations at 3,396  $\text{cm}^{-1}$ , C=O stretching vibrations at 1,731  $\text{cm}^{-1}$ , skeletal vibrations at 1,628  $\text{cm}^{-1}$ , and C-O stretching vibrations at 1,078  $\text{cm}^{-1}$ . The Raman spectrum of NGO consisted of two main features, ie, G mode at 1,594  $\text{cm}^{-1}$  and D mode at 1,347  $\text{cm}^{-1}$ . The sheet structure of NGO was observed using transmission and scanning electron

microscopy. The atomic force microscopic images showed that the thickness of NGO was about 1 nm and that the majority of the NGO sheets were approximately 10–800 nm in size. The radiochemical purity of  $^{125}\text{I}$ -NGO was greater than 94%. The  $^{125}\text{I}$ -NGO was stable in serum.

## PEG coating

Thermal gravimetric analysis of NGO and NGO-PEG was used to determine the amount of PEG coating layer on the surface of NGO (Figure 1). The decomposition temperature of PEG ranges from approximately 328°C to 439°C (data not shown). NGO-PEG undergoes an obvious weight loss above 260°C compared with NGO, indicating the presence of PEG on the surface of NGO. The mismatch of PEG weight loss around 260°C may be due to the existence of NGO and its non-uniform size. The amount of the PEG coating layer in NGO-PEG was approximately 5.8%. The degree of functionality in NGO-PEG can be calculated as a molar functionality:  $(5.8/6,000)/(94.2/12) = 0.01\%$ . The average sizes of NGO and NGO-PEG by dynamic light scattering were  $308.4 \pm 10.4$  nm (polydispersity index  $0.276 \pm 0.028$ ) and  $314.3 \pm 6.2$  nm (polydispersity index  $0.285 \pm 0.009$ ), respectively. The zeta potential of NGO and NGO-PEG was  $-32.1 \pm 3.6$  mV and  $-25.3 \pm 2.8$  mV, respectively.

## Distribution of NGO

To evaluate the in vivo behavior of NGO suspended in Milli-Q water, NGO was labeled with  $^{125}\text{I}$  by the chloramine-T method. After intravenous injection, the percentage of injected  $^{125}\text{I}$ -NGO in each organ was investigated at 10 minutes, 30 minutes, one hour, 3 hours, and 6 hours. At 10 minutes after injection, approximately 55.9% of the injected  $^{125}\text{I}$ -NGO arrived at the liver, whereas 10.0% and

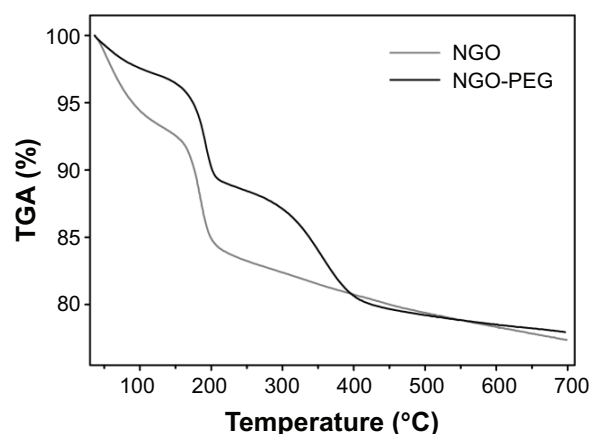


**Figure 1** TGA of NGO and NGO-PEG.

**Abbreviations:** TGA, thermal gravimetric analysis; NGO, nanoscale graphene oxide; PEG, polyethylene glycol.

2.2% reached the lung and spleen, respectively, and less than 2.0% was distributed to other organs (Figure 2A). The radioactivity in the liver and spleen decreased gradually with time, but no significant time-dependent changes were observed for the lung. The radioactivity in the liver, lung, and spleen remained at 26.9%, 6.8%, and 1.0%, respectively, at 6 hours. Meanwhile, similar studies of  $\text{Na}^{125}\text{I}$  were performed to compare the in vivo distributions of  $^{125}\text{I}$ -NGO and  $\text{Na}^{125}\text{I}$  at one hour and 6 hours (Figure 2B). It is obvious that there were significant differences between  $^{125}\text{I}$ -NGO and  $\text{Na}^{125}\text{I}$  in the liver, lung, and spleen but not in other organs. These results indicated that NGO was mainly retained in the liver, lung, and spleen. In addition, the significant differences between  $^{125}\text{I}$ -NGO and  $\text{Na}^{125}\text{I}$  demonstrated that  $^{125}\text{I}$ -NGO was stable in vivo and that the results related to the distribution of  $^{125}\text{I}$ -NGO were accurate and reliable.

Furthermore, histopathological observation was conducted 24 hours after the mice were intravenously injected with 5 mg/kg NGO through a tail vein. As shown in Figure 2C, NGO sheets accumulated in the pulmonary vascular lumen and formed larger aggregations after injection, whereas no aggregations of NGO were found in the liver or spleen.

## Influence of PEG coating on distribution of NGO

To observe the influence of the PEG coating on the in vivo distribution of NGO at early stages, the percentages of injected  $^{125}\text{I}$ -NGO in the liver, lung, and spleen at 10 minutes, 30 minutes, one hour, 3 hours, and 6 hours were compared with those of  $^{125}\text{I}$ -NGO-PEG. The results showed that the radioactivity of NGO-PEG in the liver, lung, and spleen was significantly lower than that of NGO at various time points, indicating that the PEG coating reduced the retention of NGO in these three organs (Figure 3A).

Furthermore, the blood circulation half-lives of  $^{125}\text{I}$ -NGO and  $^{125}\text{I}$ -NGO-PEG were calculated to examine the effect of the PEG coating on the pharmacokinetic profile of NGO regarding NGO distribution in the blood (Figure 3B). The blood circulation half-life of  $^{125}\text{I}$ -NGO was approximately 5.35 hours, whereas that of  $^{125}\text{I}$ -NGO-PEG was approximately 6.29 hours, indicating that the PEG coating prolonged the blood circulation half-life of NGO. The volume of distribution of  $^{125}\text{I}$ -NGO was about 0.93 L/kg, whereas that of  $^{125}\text{I}$ -NGO-PEG was approximately 0.78 L/kg. The areas under curve for  $^{125}\text{I}$ -NGO and  $^{125}\text{I}$ -NGO-PEG

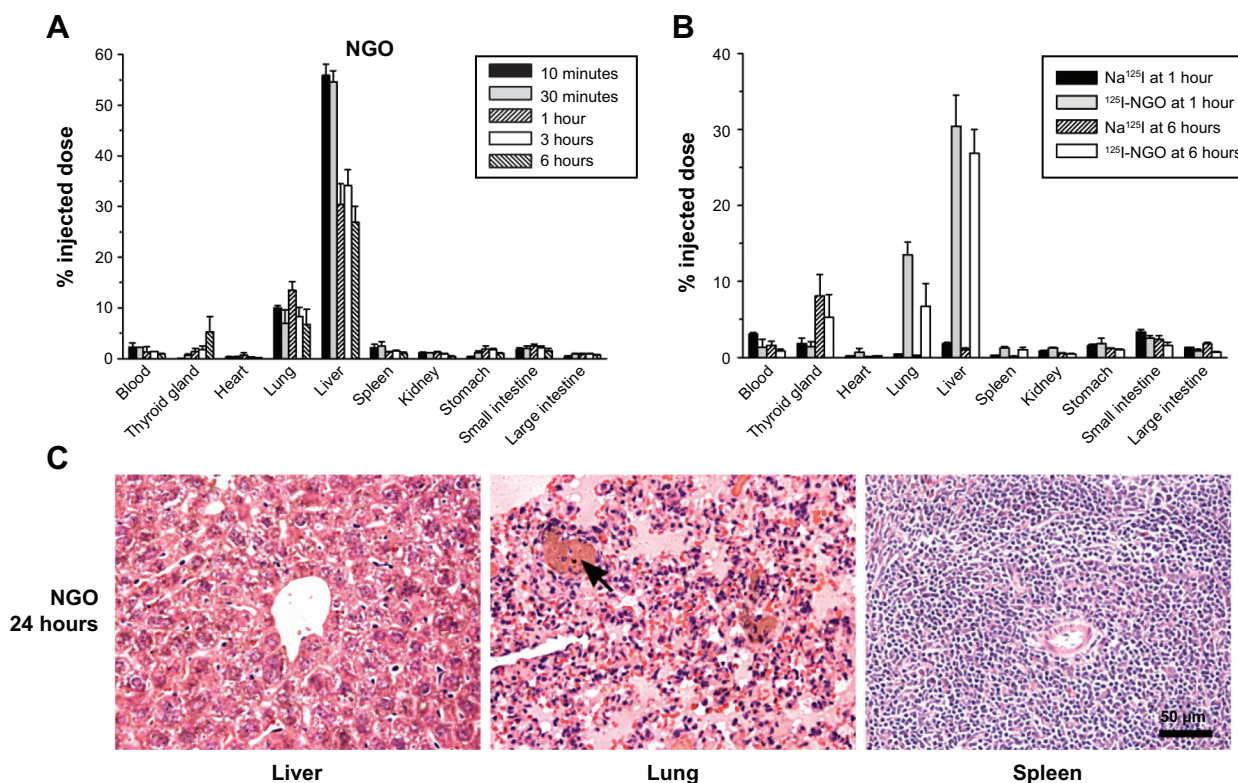


**Figure 2** Distribution of NGO after intravenous injection.

**Notes:** (A) Distribution of  $^{125}\text{I}$ -NGO in the blood and main organs of mice at different time points. (B) Comparative distribution of  $\text{Na}^{125}\text{I}$  and  $^{125}\text{I}$ -NGO in mice at one and 6 hours ( $n=5$  in each group). Values are presented as the mean  $\pm$  standard error of the mean. (C) Distribution of NGO in sections of organs, including the liver, lung, and spleen, after 24 hours. The black arrow indicates NGO aggregations. All of the images are shown at 400 $\times$  magnification with a 50  $\mu\text{m}$  scale bar.

**Abbreviation:** NGO, nanoscale graphene oxide.



were about 0.17 mg-min/mL and about 0.23 mg-min/mL, respectively.

## Influence of PEG coating on clearance of NGO

The influence of the PEG coating on the long-term fate of NGO was examined by histopathological observation of the main

organs, including the liver, lung, and spleen, 3 months after injection (Figure 3C). The number of NGO aggregations in the liver, lung, and spleen from NGO-PEG-treated mice was significantly reduced compared with such aggregations in NGO-treated mice, indicating that the PEG coating promoted clearance of NGO from these organs. However, this observation also suggested the persistence of NGO and NGO-PEG after 3 months.

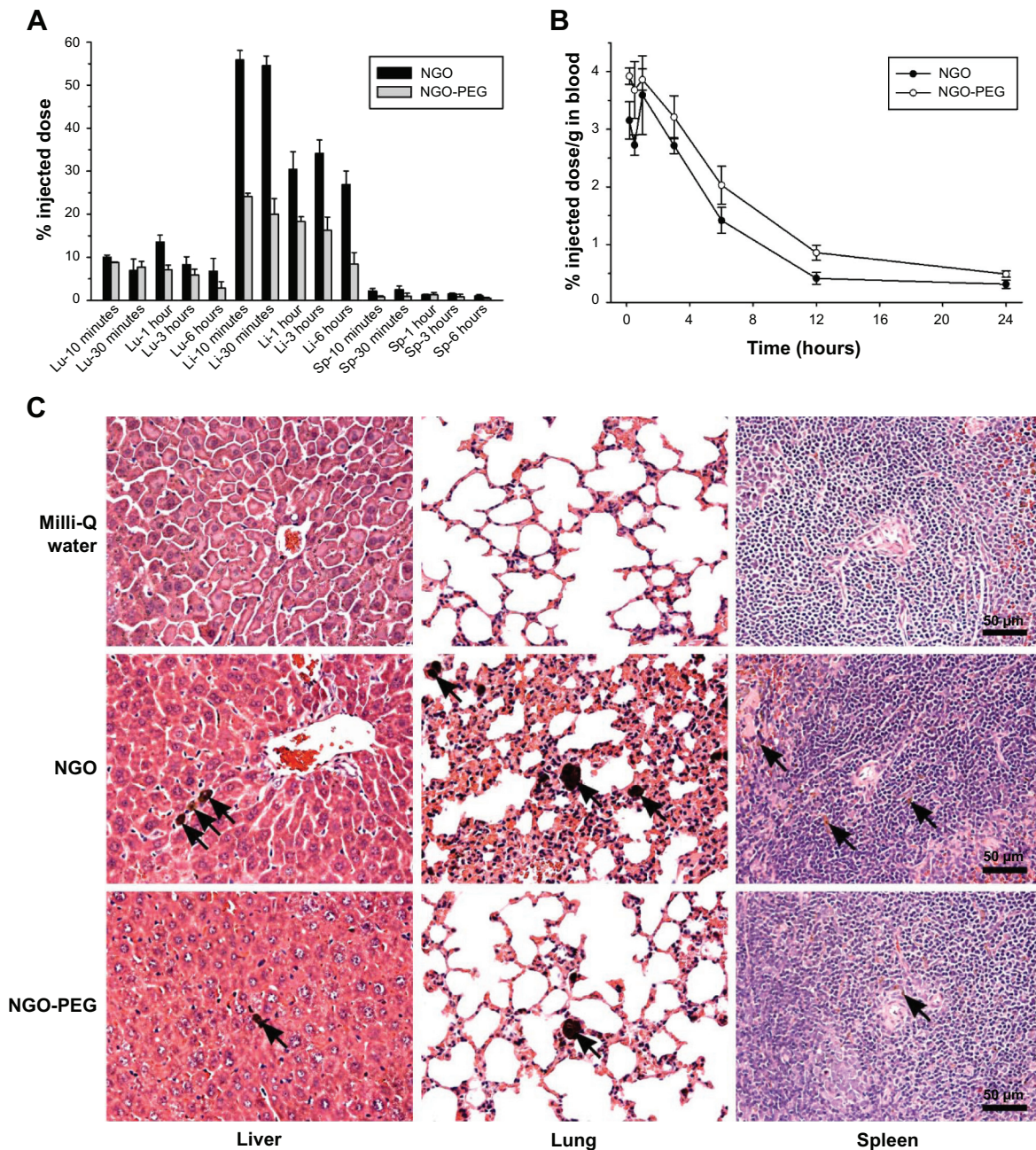


**Figure 3** Influence of PEG coating on distribution of NGO.

**Notes:** (A) Comparative distribution of  $^{125}\text{I}$ -NGO and  $^{125}\text{I}$ -NGO-PEG in the lung (Lu), liver (Li), and spleen (Sp) at different time points. (B) Blood circulation curves of  $^{125}\text{I}$ -NGO and  $^{125}\text{I}$ -NGO-PEG in mice within 24 hours ( $n=5$  in each group). Values are presented as the mean  $\pm$  standard error of the mean. (C) Distributions of NGO and NGO-PEG in sections of organs, including the liver, lung, and spleen, after 3 months. The black arrows indicate NGO aggregations. All of the images are shown at 400 $\times$  magnification with a 50  $\mu$ m scale bar.

**Abbreviations:** NGO, nanoscale graphene oxide; PEG, polyethylene glycol.

## Influence of PEG coating on toxicity of NGO

First, the body weights of the mice in these three groups were investigated at various time points. The results showed that NGO caused an early decrease in body weight after 24 hours, whereas PEG significantly improved the NGO-induced weight loss (Figure 4). The body weights of all mice then increased slightly without statistically significant differences between the three groups at each time point until 3 months.

To obtain detailed information regarding the influence of NGO and NGO-PEG on important organs, a blood biochemical analysis was performed (Figure 5). NGO induced an increase in alanine aminotransferase, aspartate aminotransferase, and creatinine after 24 hours, indicating the occurrence of acute injury to organs including the liver and kidney. The PEG coating significantly reduced these indices back to normal levels, indicating that the PEG coating effectively alleviated NGO-induced acute injury to these organs.

Given the results of the distribution and blood biochemical analyses, histopathological changes in the liver, lung, spleen, and kidney were evaluated at early stages (Figure 6). Lung tissue treated with NGO exhibited damage to the alveolar architecture, moderate pulmonary parenchymal edema, neutrophil infiltration, congestion, and hemorrhage accompanied by NGO aggregations after 24 hours, indicating the occurrence of acute lung injury. With the PEG coating, the NGO-induced acute inflammatory responses were improved significantly, but NGO aggregations were still observed in sections of the lung. Moreover, NGO also induced early hepatic injuries characterized by the massive ballooning

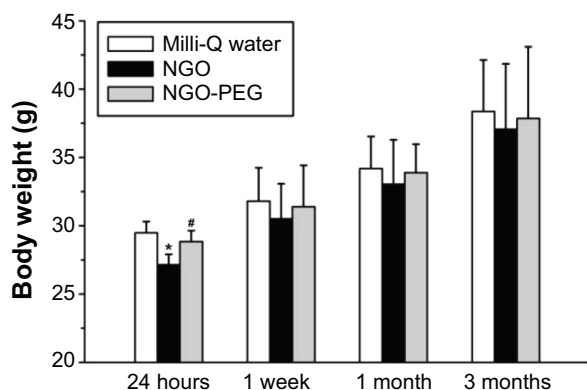


**Figure 4** Body weights of mice treated with Milli-Q water, 5 mg/kg NGO, or 5 mg/kg NGO-PEG and sacrificed at 24 hours, one week, one month, and 3 months (n=5 in each group).

**Notes:** Values are presented as the mean  $\pm$  standard error of the mean. \*Values that differed significantly from the Milli-Q group at  $P < 0.05$ . #Values that differed significantly from the NGO group at  $P < 0.05$ .

**Abbreviations:** NGO, nanoscale graphene oxide; PEG, polyethylene glycol.

degeneration and necrosis of hepatocytes surrounding the central vein, which could be alleviated by PEG coating of NGO. However, there were no obvious pathological changes in the spleen and kidneys of mice treated with either NGO or NGO-PEG after 24 hours (data not shown).

The acute liver and lung injuries induced by NGO were subsequently gradually alleviated and became chronic inflammatory responses over time (Figure 7). The chronic pathological changes in these organs were assessed by standard hematoxylin-eosin and Masson trichrome staining after 3 months (Figure 8). Compared with the Milli-Q water group, the liver and lung tissues of the group treated with NGO exhibited much more collagen deposition and tissue injury, indicating that NGO induced chronic hepatic and lung fibrosis. The NGO-induced chronic pathological changes in the liver and lung may originate from the acute hepatic and lung injuries discussed above. However, PEG coating significantly improved the NGO-induced chronic hepatic and lung fibrosis characterized by reduced collagen deposition. There were no chronic pathological changes observed in the spleen and kidneys after 3 months in either group (data not shown).

## Discussion and conclusion

NGO is a promising new nanomaterial for drug delivery and tumor treatment. However, the *in vivo* distribution and toxicity of NGO has rarely been evaluated, even though these issues are critical for assessing the potential biomedical applications of NGO. Furthermore, the influence of a PEG coating on the distribution and toxicity of NGO has not been reported until now. In this study, we examined the *in vivo* behavior and toxicology of NGO in mice after intravenous injection. The influence of the PEG coating on the distribution and toxicity of NGO was investigated. The results showed that NGO particles with a size range of 10–800 nm were mainly retained in the liver, lung, and spleen. Retention in the lung was partially due to NGO aggregation. PEG coating reduced the retention of NGO in the liver, lung, and spleen, and promoted clearance of NGO from these organs, but NGO and NGO-PEG were still present after 3 months. Moreover, the PEG coating effectively reduced the early weight loss caused by NGO and alleviated NGO-induced acute tissue injuries, which can include damage to the liver, lung, and kidney, and chronic hepatic and lung fibrosis.

It is well known that the reticuloendothelial system or the MPS is responsible for the retention of nanoparticles in tissues or organs.<sup>25</sup> In the present study, retention of NGO in the

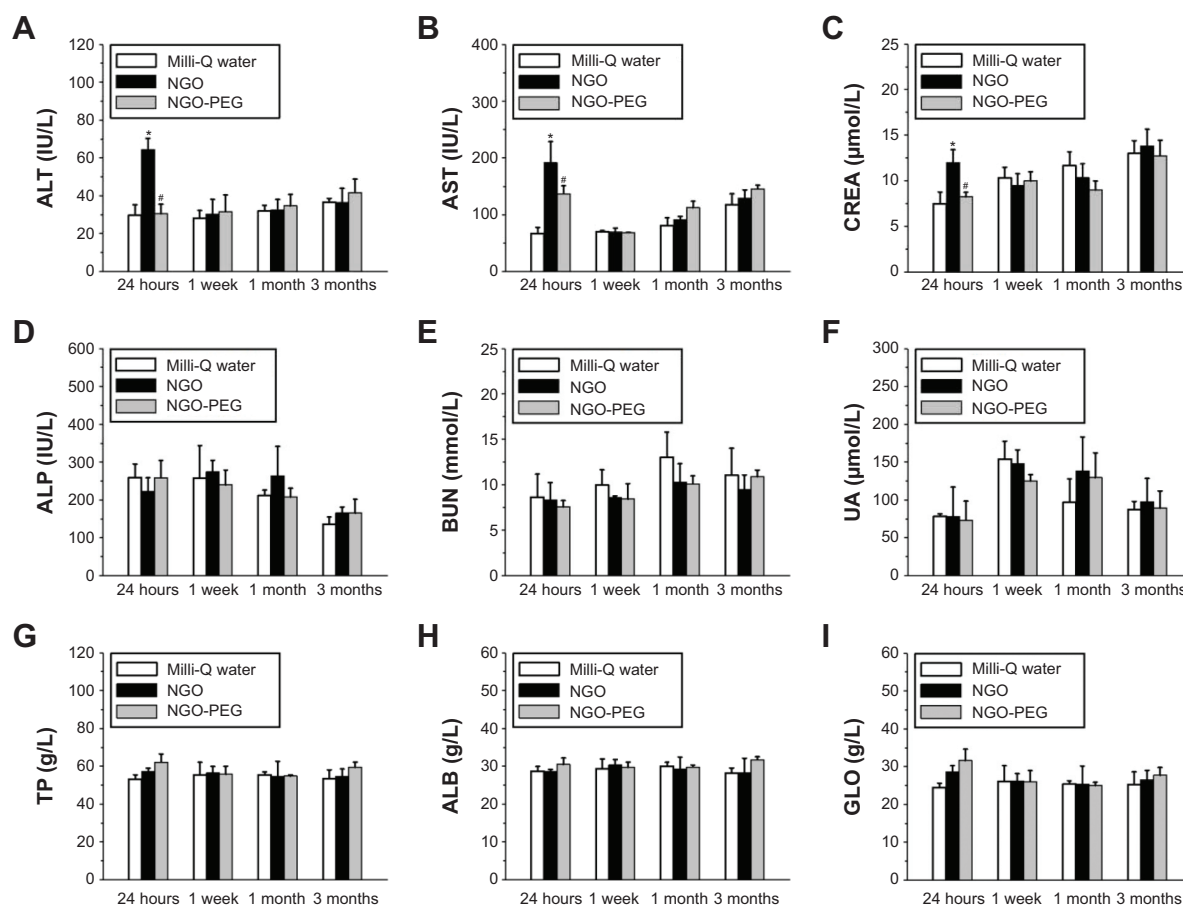


**Figure 5** Blood biochemistry analysis of mice treated with Milli-Q water, 5 mg/kg NGO, or 5 mg/kg NGO-PEG and sacrificed at 24 hours, one week, one month, and 3 months.

**Notes:** (A–I) Serum levels of ALT, AST, CREA, ALP, BUN, UA, TP, ALB, and GLO were evaluated ( $n=5$  in each group). The values are presented as the mean  $\pm$  standard error of the mean. \*Values that differed significantly from Milli-Q group at  $P<0.05$ . #Values that differed significantly from NGO group at  $P<0.05$ .

**Abbreviations:** ALT, alanine aminotransferase; AST, aspartate aminotransferase; CREA, creatinine; ALP, alkaline phosphatase; BUN, blood urea nitrogen; UA, uric acid; TP, total protein; ALB, albumin; GLO, globulin; NGO, nanoscale graphene oxide; PEG, polyethylene glycol.

liver, lung, and spleen may be attributed to its uptake by the reticuloendothelial system or MPS. However, accumulation of NGO in the lung exhibited different time-related changes from the accumulation in the liver and spleen, implying the possibility of other mechanisms. Considering the size range of NGO from 10 nm to 800 nm, the biodistribution, pharmacokinetics, and toxicity of NGO sheets with small and large sizes may be different. NGO sheets with small sizes can pass through the kidneys into urine and be rapidly eliminated by a renal route without obvious toxicity. Meanwhile, NGO sheets with large sizes may form aggregations or be captured by the MPS with obvious toxicity. The results of the histopathological observation demonstrated that blocking of the pulmonary blood vessels by NGO aggregations was partially responsible for retention of NGO in the lung.

In this study, the PEG coating was accomplished by absorption rather than covalent binding between NGO and PEG.<sup>26</sup> The adsorption of PEG on the surface of

NGO might be a consequence of hydrogen bonds, Van der Waals forces, and other weak interactions. The PEG coating may reduce retention of NGO in the liver, lung, and spleen by providing steric hindrance that prevents protein binding and effectively decreases MPS uptake and formation of NGO aggregation.<sup>27</sup> Furthermore, the PEG coating increased the blood concentration of NGO at each time point and prolonged the blood circulation half-life of NGO due to the reduced MPS uptake and formation of NGO aggregation.

With respect to the long-term fate of NGO, the results of the histopathological observation show that the PEG coating promoted clearance of NGO from the liver, lung, and spleen, which may also be due to the reduced MPS uptake of NGO. NGO of smaller sizes may be quickly eliminated via the renal route, whereas NGO of larger sizes and NGO aggregates may be taken up by macrophages and cleared through the biliary pathway into the feces or by other mechanisms.<sup>28</sup> However,



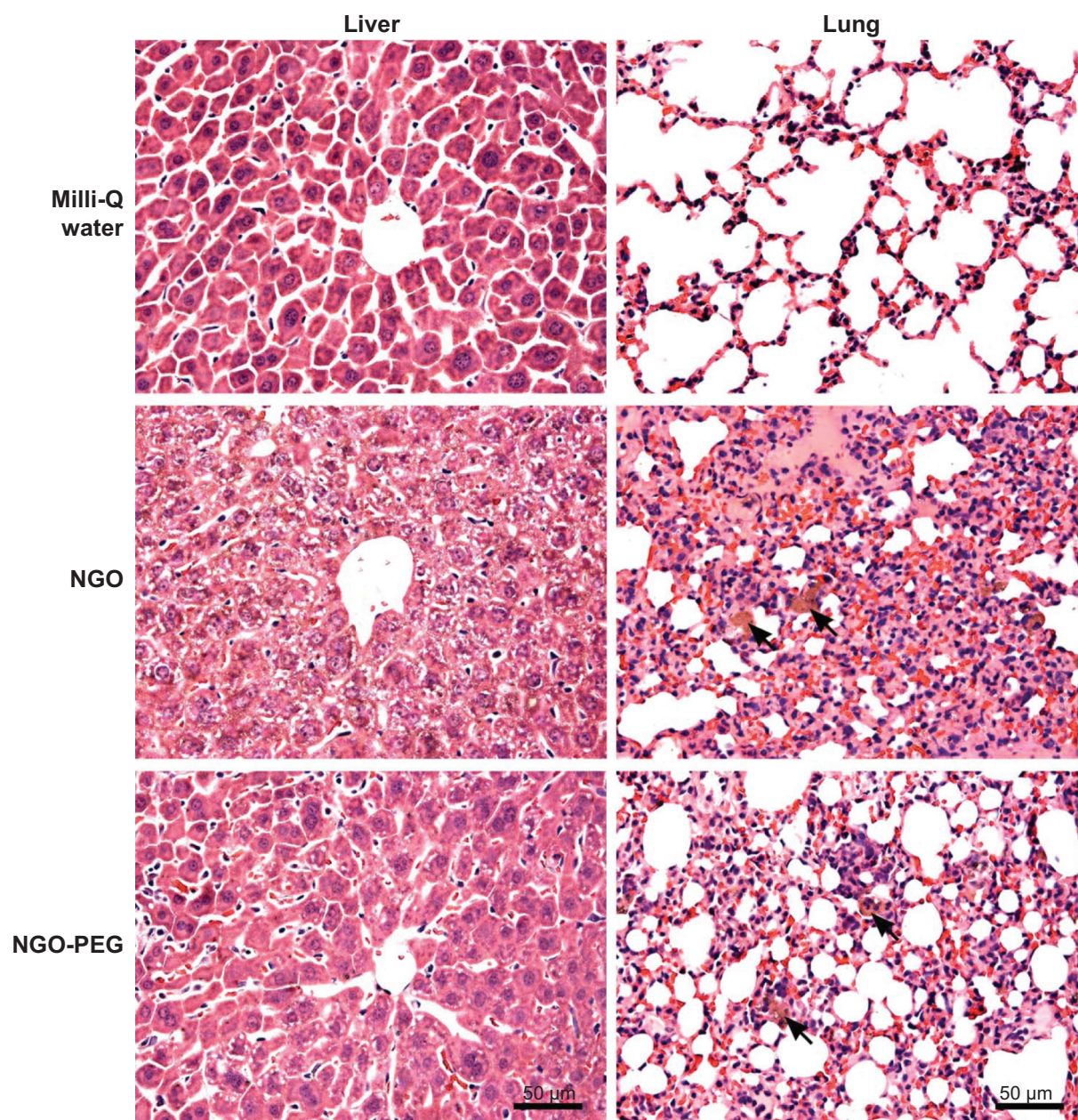


**Figure 6** Acute histopathological changes induced by NGO and NGO-PEG.

**Notes:** Representative HE-stained images of major organs after 24 hours, including the liver and lung, collected from mice treated with Milli-Q water, 5 mg/kg NGO, or 5 mg/kg NGO-PEG. The black arrows indicate NGO aggregations. All of the images are shown at 400× magnification with a 50 µm scale bar.

**Abbreviations:** HE, hematoxylin-eosin; NGO, nanoscale graphene oxide; PEG, polyethylene glycol.

the long-term existence of NGO and NGO-PEG in these organs may be due to the large numbers of NGO aggregations and the limited NGO clearance ability of the organism.

In the present study, the influence of the PEG coating on the toxicity of NGO was determined using an evaluation system that included assessment of body weight, a blood biochemical analysis, and a histopathological examination. A relatively low dose of NGO (5 mg/kg) was chosen because of the increased mortality in mice that received a higher dose of NGO in the preliminary experiment, which may have been

due to dyspnea resulting from blocking of the pulmonary blood vessels by NGO aggregations. NGO-induced effects, such as early weight loss, acute injury to tissues including the liver, lung, and kidney, and chronic hepatic and lung fibrosis, may be closely related to the physiochemical characteristics and distribution of NGO. NGO may interfere with the normal physiological function of important organs, such as the liver and lung, resulting in acute and chronic toxicity. However, PEG could effectively eliminate the NGO-induced side effects by regulating the *in vivo* behavior of NGO.



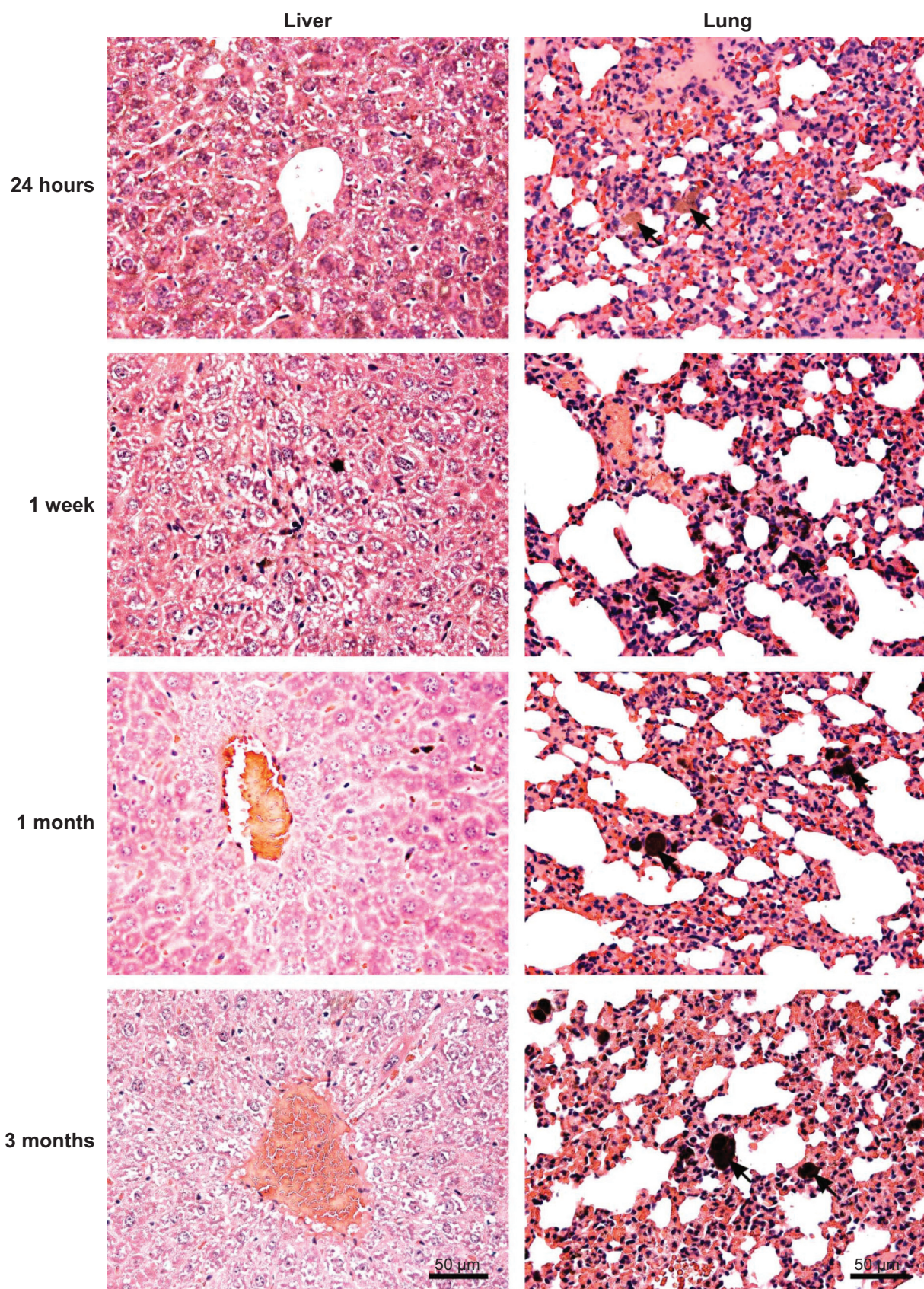


**Figure 7** Time-dependent histopathological changes induced by NGO.

**Notes:** Representative HE-stained images of the liver and lung collected from mice treated with 5 mg/kg NGO at 24 hours, one week, one month, and 3 months. The black arrows indicate NGO aggregations. All of the images are shown at 400× magnification with a 50 µm scale bar.

**Abbreviations:** NGO, nanoscale graphene oxide; HE, hematoxylin-eosin.



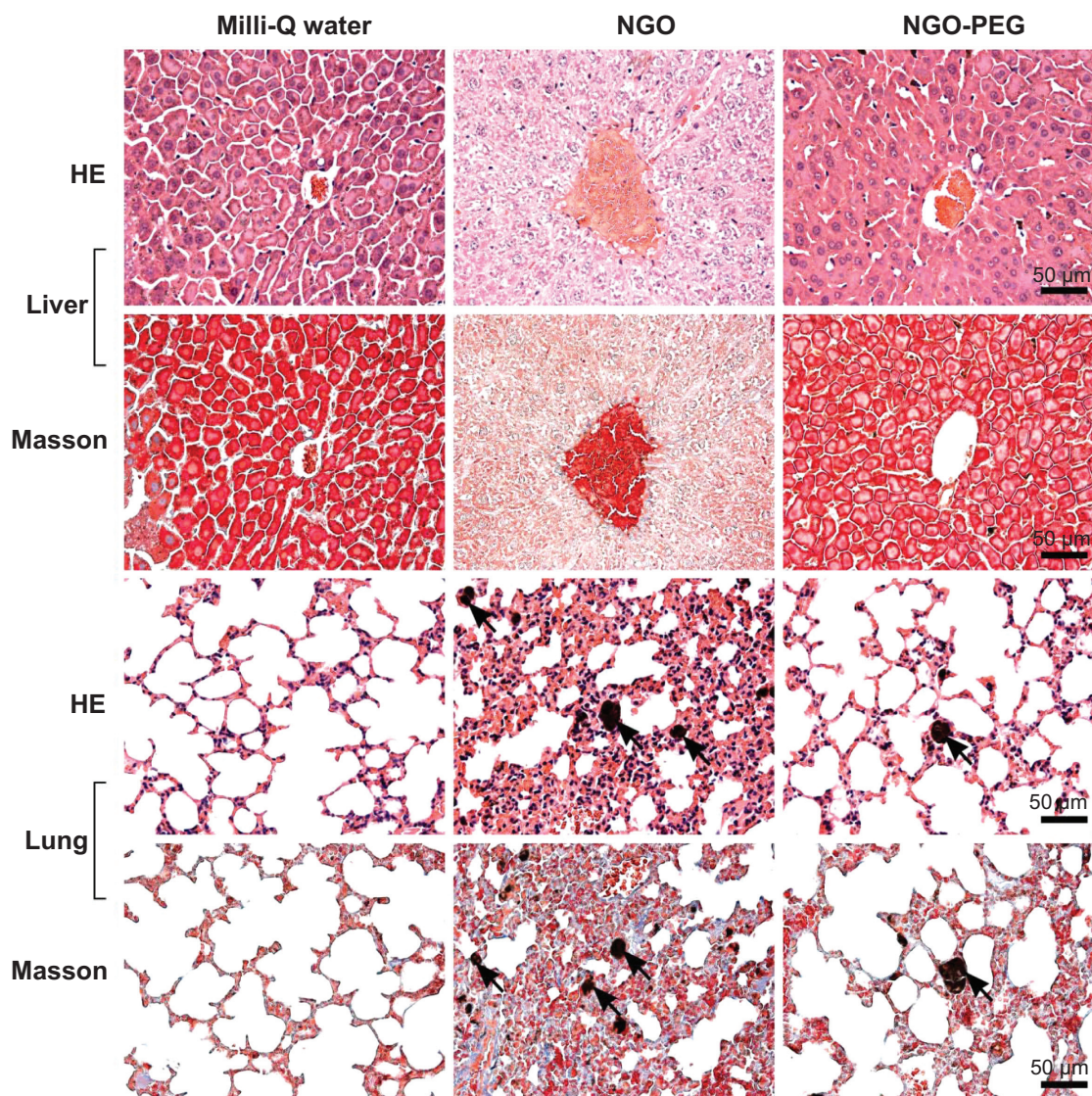


**Figure 8** Chronic histopathological changes induced by NGO and NGO-PEG.

**Notes:** Representative HE and Masson-stained images of the liver and lung, collected from mice treated with Milli-Q water, 5 mg/kg NGO, or 5 mg/kg NGO-PEG and sacrificed after 3 months. The black arrows indicate NGO aggregations. All of the images are shown at 400× magnification with a 50 µm scale bar.

**Abbreviations:** NGO, nanoscale graphene oxide; HE, hematoxylin-eosin; PEG, polyethylene glycol.

There have been several studies of the *in vivo* distribution and toxicity of NGO after intravenous injection, and their results have shown some differences from those of our study. Zhang et al demonstrated that NGO (10–800 nm, suspended in phosphate-buffered saline) was predominantly deposited in the lungs, resulting in pulmonary toxicity at a dosage of 10 mg/kg body weight.<sup>29</sup> Yang et al reported that PEGylated NGO (10–30 nm, suspended in water) accumulated in the reticuloendothelial system, including in the liver and spleen, and did not cause appreciable toxicity at a dosage of 20 mg/kg.<sup>30</sup> In this study, NGO (10–800 nm, suspended in Milli-Q water) was mainly retained in the liver, lung, and spleen, with acute and chronic toxicity, whereas the PEG

coating reduced the retention of NGO and alleviated NGO-induced toxicity. Based on the analysis of our work and previous studies, the distribution of NGO appears to be closely related to its size and dispersion. Because the distribution of nanoparticles determines the toxic responses induced in organs, NGO of different sizes and dispersions show various results in terms of biocompatibility and toxicity.

In conclusion, the PEG coating was able to reduce retention of NGO in the liver, lung, and spleen, promote clearance of NGO from these organs, and alleviate NGO-induced acute and chronic toxicity. These results provide powerful evidence for future biomedical application of NGO. However, further toxicology studies are required. Future studies should

concentrate on the influence of the physiochemical characteristics of NGO, including size, dispersion, and oxidative states, on the distribution and toxicity of NGO.

## Acknowledgments

This work was supported by grants from the National Science Foundation of China (10775169, 10905086, 10975179), the Shanghai Municipal Natural Science Foundation (08ZR1422700, 08JC1422600), the Ministry of Health (2009ZX10004-301), the CAS Innovation Program (095501K), and the MOST973 Program (2006CB705605). The funders had no role in the study design, data collection and analysis, decision to publish, or preparation of the manuscript.

## Disclosure

The authors report no financial or other conflicts of interest relevant to the subject of this paper.

## References

- Shan CS, Yang HF, Han DX, Zhang QX, Ivaska A, Niu L. Water-soluble graphene covalently functionalized by biocompatible poly-L-lysine. *Langmuir*. 2009;25:12030–12033.
- Xiao LQ, Liao LQ, Liu LJ. Chemical modification of graphene oxide with carbethoxycarbene under microwave irradiation. *Chem Phys Lett*. 2013;556:376–379.
- Wu CK, Wang GJ, Dai JF. Controlled functionalization of graphene oxide through surface modification with acetone. *J Mater Sci*. 2013;48:3436–3442.
- Bustos-Ramirez K, Martinez-Hernandez AL, Martinez-Barrera G, de Icaza M, Castano VM, Velasco-Santos C. Covalently bonded chitosan on graphene oxide via redox reaction. *Materials*. 2013;6(3):911–926.
- Bai YC, Rakhi RB, Chen W, Alshareef HN. Effect of pH-induced chemical modification of hydrothermally reduced graphene oxide on supercapacitor performance. *J Power Sources*. 2013;233:313–319.
- Liu ZA, Feng LZ. Graphene in biomedicine: opportunities and challenges. *Nanomedicine*. 2011;6:317–324.
- Kavitha T, Kang IK, Park SY. Poly(acrylic acid)-grafted graphene oxide as an intracellular protein carrier. *Langmuir*. 2014;30:402–409.
- Wu SL, Zhao XD, Cui ZG, et al. Cytotoxicity of graphene oxide and graphene oxide loaded with doxorubicin on human multiple myeloma cells. *Int J Nanomedicine*. 2014;9:1413–1421.
- Tu Q, Pang L, Chen Y, et al. Effects of surface charges of graphene oxide on neuronal outgrowth and branching. *Analyst*. 2014;139:105–115.
- Zhang M, Le HN, Ye BC. Graphene oxide-based fluorescent “on/off” switch for visual bioassay using “molecular beacon”-hosted Hoechst dyes. *ACS Appl Mater Interface*. 2013;5:8278–8282.
- Wang H, Gu W, Xiao N, Ye L, Xu QY. Chlorotoxin-conjugated graphene oxide for targeted delivery of an anticancer drug. *Int J Nanomedicine*. 2014;9:1433–1442.
- Wang HX, Sun DM, Zhao NN, et al. Thermo-sensitive graphene oxide-polymer nanoparticle hybrids: synthesis, characterization, biocompatibility and drug delivery. *J Mater Chem B*. 2014;2:1362–1370.
- Lim DJ, Sim M, Oh L, Lim K, Park H. Carbon-based drug delivery carriers for cancer therapy. *Arch Pharm Res*. 2014;37:43–52.
- Ernsting MJ, Tang WL, MacCallum NW, Li SD. Preclinical pharmacokinetic, biodistribution, and anti-cancer efficacy studies of a docetaxel-carboxymethylcellulose nanoparticle in mouse models. *Biomaterials*. 2012;33:1445–1454.
- Bao YJ, Jin Y, Chivukula P, et al. Effect of PEGylation on biodistribution and gene silencing of siRNA/lipid nanoparticle complexes. *Pharm Res*. 2013;30:342–351.
- Shah NB, Vercellotti GM, White JG, Fegan A, Wagner CR, Bischof JC. Blood-nanoparticle interactions and in vivo biodistribution: impact of surface PEG and ligand properties. *Mol Pharm*. 2012;9:2146–2155.
- Lu F, Doane TL, Zhu JJ, Burda C. A method for separating PEGylated Au nanoparticle ensembles as a function of grafting density and core size. *Chem Commun*. 2014;50:642–644.
- Tobin LA, Xie YL, Tsokos M, et al. Pegylated siRNA-loaded calcium phosphate nanoparticle-driven amplification of cancer cell internalization in vivo. *Biomaterials*. 2013;34:2980–2990.
- Lak A, Dieckhoff J, Ludwig F, et al. Highly stable monodisperse PEGylated iron oxide nanoparticle aqueous suspensions: a nontoxic tracer for homogeneous magnetic bioassays. *Nanoscale*. 2013;5:11447–11455.
- Chaudhari KR, Ukawala M, Manjappa AS, et al. Opsonization, biodistribution, cellular uptake and apoptosis study of PEGylated PBCA nanoparticle as potential drug delivery carrier. *Pharm Res*. 2012;29:53–68.
- Ernsting MJ, Murakami M, Roy A, Li SD. Factors controlling the pharmacokinetics, biodistribution and intratumoral penetration of nanoparticles. *J Control Release*. 2013;172:782–794.
- Brannon-Peppas L, Blanchette JO. Nanoparticle and targeted systems for cancer therapy. *Adv Drug Deliv Rev*. 2012;64:206–212.
- Yang K, Zhang S, Zhang G, Sun X, Lee ST, Liu Z. Graphene in mice: ultrahigh in vivo tumor uptake and efficient photothermal therapy. *Nano Lett*. 2010;10:3318–3323.
- Li B, Yang JZ, Huang Q, et al. Biodistribution and pulmonary toxicity of intratracheally instilled graphene oxide in mice. *NPG Asia Materials*. 2013;5.
- Duan XP, Li YP. Physicochemical characteristics of nanoparticles affect circulation, biodistribution, cellular internalization, and trafficking. *Small*. 2013;9:1521–1532.
- In I, Park YJ, Park SY. Preparation of water soluble graphene using polyethylene glycol: comparison of covalent approach and noncovalent approach. *Journal of Industrial and Engineering Chemistry*. 2011;17:298–303.
- Prantner AM, Scholler N. Biological barriers and current strategies for modifying nanoparticle bioavailability. *J Nanosci Nanotechnol*. 2014;14:115–125.
- Jones SW, Roberts RA, Robbins GR, et al. Nanoparticle clearance is governed by Th1/Th2 immunity and strain background. *J Clin Invest*. 2013;123:3061–3073.
- Zhang XY, Yin JL, Peng C, et al. Distribution and biocompatibility studies of graphene oxide in mice after intravenous administration. *Carbon*. 2011;49:986–995.
- Yang K, Wan J, Zhang S, Zhang Y, Lee ST, Liu Z. In vivo pharmacokinetics, long-term biodistribution, and toxicology of PEGylated graphene in mice. *ACS Nano*. 2011;5:516–522.

### International Journal of Nanomedicine

### Publish your work in this journal

The International Journal of Nanomedicine is an international, peer-reviewed journal focusing on the application of nanotechnology in diagnostics, therapeutics, and drug delivery systems throughout the biomedical field. This journal is indexed on PubMed Central, MedLine, CAS, SciSearch®, Current Contents®/Clinical Medicine,

Submit your manuscript here: <http://www.dovepress.com/international-journal-of-nanomedicine-journal>

### Dovepress

Journal Citation Reports/Science Edition, EMBase, Scopus and the Elsevier Bibliographic databases. The manuscript management system is completely online and includes a very quick and fair peer-review system, which is all easy to use. Visit <http://www.dovepress.com/testimonials.php> to read real quotes from published authors.